Dynamics of laser-ablation Ti plasmas studied by laser-induced fluorescence imaging spectroscopy

K. Sasaki,[a] S. Matsui, H. Ito, and K. Kadota
Department of Electronics, Nagoya University, Nagoya 464-8603, Japan

(Received 5 July 2002; accepted 9 September 2002)

The distributions of Ti^+ and Ti densities in laser-ablation Ti plasmas were visualized by laser-induced fluorescence imaging spectroscopy. The absolute Ti density was determined by ultraviolet absorption spectroscopy. The absolute Ti^+ density was evaluated by comparing the laser-induced fluorescence intensity from Ti^+ with that from Ti. In addition, we evaluated the total numbers of Ti^+ and Ti in plasmas by integrating the density distributions spatially. As a result, it was found that the total number of Ti^+ was higher than that of Ti in the initial stage of laser-ablation plasmas. In ambient He gas, we observed the temporal increase in the total number of Ti, indicating the gas-phase production of Ti due to neutralization of Ti^+. The increase in the total number of Ti^+ was also observed, suggesting the production of Ti^+ due to neutralization of Ti^{2+}. The present experimental results show that Ti^+ and Ti^{2+} are major species produced by laser ablation of a metal Ti target. © *2002 American Institute of Physics.* [DOI: 10.1063/1.1518135]
PACS: 52.38.Mf, 52.70.Kz, 81.15.Fg

I. INTRODUCTION

High-density plasmas produced by laser ablation of solid targets have various applications such as laser-induced mass analysis, laser-induced breakdown spectroscopy, light sources including x-ray laser mediums, synthesis of nanoclusters, and thin-film deposition. In particular, thin-film deposition called pulsed laser deposition (PLD) is the most important application from the industrial point of view. Although thin films of various materials have been produced by the PLD technique, a better understanding of laser-ablation plasmas is required for the improvement of deposition characteristics.

For a better understanding of the PLD technique, what we should know first is species ejected from the target material by laser ablation. Since particles ejected from the target expand into vacuum or ambient gas rapidly, the particle densities in laser-ablation plasmas have dynamic variations both temporally and spatially. Accordingly, it is important to measure the temporal variations of spatial distributions of particle densities in plasmas with high-temporal and spatial resolutions. The dynamic variations of particle densities are affected by hydrodynamic interactions between ejected particles and ambient gas. Ionization, neutralization, and chemical reactions in plasmas also influence the temporal and spatial variations of particle densities. The spatial distributions of particle densities are helpful information for determining the separation distance between the target and the substrate in the PLD technique.

Recently, Ti-based thin films such as TiO_2 and TiN, which can be synthesized by the PLD technique,[1–4] have attracted the interest of many researchers. In the present work, we measured the spatial distributions of Ti^+ and Ti densities in Ti plasmas produced by laser ablation of a metal Ti target in ambient He gas, in order to understand basic characteristics of laser-ablation Ti plasmas. We employed laser-induced fluorescence (LIF) imaging spectroscopy[5–8] which visualized the distributions of Ti^+ and Ti densities in plasmas with high-temporal resolutions. The absolute Ti density was determined by ultraviolet absorption spectroscopy (UVAS). The absolute Ti^+ density was evaluated from the ratio of LIF intensity from Ti^+ to that from Ti. By calculating the total numbers of Ti^+ and Ti in plasmas, we discussed the influence of gas-phase reactions separately from hydrodynamic effects. As a result, it has been found that Ti^+ and Ti^{2+} are the major species ejected from the metal Ti target by laser ablation. In addition, we have shown that neutralization of Ti^+ plays an important role in the gas-phase production of Ti in laser-ablation Ti plasmas.

II. EXPERIMENT

A. Laser-ablation system

We used a simple laser-ablation system shown in Fig. 1. A metal Ti target was installed in a vacuum chamber which was evacuated below 5×10^{-7} Torr using a turbomolecular pump. The target was fixed on a rotating holder to disperse the ablation point. Nd:YAG laser pulses at a wavelength of 1.06 μm irradiated the target from the normal direction to the target surface. The repetition rate and the duration of the YAG laser pulse were 10 Hz and 10 ns, respectively. The YAG laser beam was focused using a lens, so that the fluence of the YAG laser pulse on the target surface was approximately 1.5 J/cm^2. The diameter of the YAG laser beam on the target surface was approximately 1 mm. The present experiment was carried out in vacuum and in ambient He gas at pressures less than 1.5 Torr.

[a]Electronic mail address: sasaki@nuee.nagoya-u.ac.jp

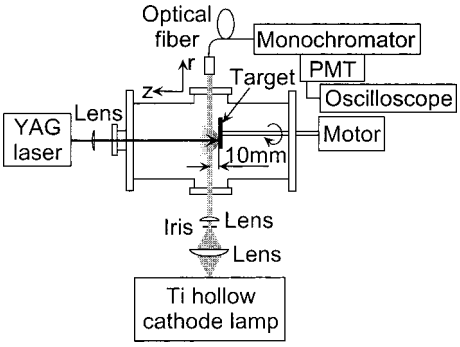

FIG. 1. Schematic of the laser ablation and UVAS systems.

B. Laser-induced fluorescence imaging spectroscopy

The densities of Ti^+ and Ti in plasmas were measured by LIF imaging spectroscopy.[5–8] The details of LIF imaging spectroscopy have been described in a previous paper.[5] Briefly, tunable laser pulses yielded from an optical parametric oscillator (OPO) were injected into plasmas in front of the target. The tunable laser beam had a plane shape with a width of 27 mm (in the perpendicular direction to the target surface) and a thickness of 1 mm (in the parallel direction to the target surface). The wavelengths of the OPO laser were tuned to excite Ti and Ti^+ in plasmas. Excited Ti and Ti^+ yielded fluorescences on the plane-shaped OPO laser beam. We took the images of fluorescences using a charge-coupled camera with a gated image intensifier. Interference filters were used to separate the fluorescences from stray lights and self emissions of plasmas. In this way, we visualized the density distributions of Ti and Ti^+ in plasmas. The temporal variations of the density distributions were obtained by changing the delay time t_D between the oscillations of YAG and OPO lasers. The energy levels and wavelengths used in the present experiment are listed in Table I.[9,10]

In general, the LIF intensity is reduced when the frequency of collisional quenching is comparable to the reciprocal of the radiative lifetime of the laser-excited state.[11] In the present experimental condition, it has been confirmed that collision with ambient He gas does not affect the LIF intensities of Ti and Ti^+. On the other hand, collision with particles ejected from the target reduced the lifetime of laser-excited Ti with a factor of ~ 1.5 at $t_D \leqslant 20$ μs. The lifetime of Ti^+ was not affected by collision with ejected particles. Another problem of LIF imaging spectroscopy is the reduction in the excitation efficiency due to the Doppler effect. This problem becomes serious when Ti and Ti^+ have fast velocity in parallel direction to the OPO laser beam. In the present experimental configuration, the Doppler effect resulted in the low sensitivity in the wing part of the density distribution at the initial stage. The influence of the Doppler effect examined experimentally will be described in the appendix.

TABLE I. Energy levels and wavelengths used in LIF imaging spectroscopy.

Particle	Initial state	Excitation	Excited state	Fluorescence	Final state
Ti^+	$a^4F_{3/2}$	324.198 nm →	$z^{F^\circ}_{3/2}$	334.03 nm →	$b^4F_{3/2}$
Ti	a^3F_2	293.353 nm →	$v^{F^\circ}_3$	445.53 nm →	b^3F_3

C. Ultraviolet absorption spectroscopy

The LIF imaging spectroscopy described above does not provide us with the absolute densities of Ti^+ and Ti. In the present work, we determined the absolute Ti density by UVAS. The system for UVAS is schematically shown in Fig. 1. The resonance emission at a wavelength of 363.55 nm ($a^3F_2 \leftarrow y^3G^\circ_3$) obtained from a hollow cathode Ti lamp was injected into plasmas. The Ti lamp emission transmitted through the plasma was detected using a monochromator and a photomultiplier tube. A conventional theory[12] was used to evaluate the line-integrated Ti density from absorption in the plasma. Since absorption immediately after the irradiation of the YAG laser pulse was close to unity, we evaluated the absolute Ti density from absorption at $t_D \geqslant 1.5$ ms when absorption less than 80% was observed. The local Ti density was evaluated from the line-integrated density by comparing it with the distribution of relative Ti density measured by LIF imaging spectroscopy.

The error in the absolute Ti density determined by UVAS is owing to the ambiguity in absorption, the error in the transition probability,[10] the ambiguity in the estimation of the temperatures of Ti atoms in the ablation plasma and in the hollow cathode lamp, and the random noise superposed on the signal. The ambiguity in absorption due to scattering and background absorption was proved to be negligible by repeating the same measurement at a wavelength of 359.4 nm which was obtained from Ne in the same hollow cathode lamp. The temperature of Ti in the ablation plasma was assumed to be 300 K, which may be reasonable since the absorption measurement was carried out at $t_D \geqslant 1.5$ ms in ambient He gas. Considering other sources of the error, the error in the absolute Ti atom density determined by UVAS was estimated to be less than a factor of 2.

The absolute Ti^+ density was determined by comparing the LIF intensity from Ti^+ with that from Ti.[13] When the OPO laser beam was injected into the plasma without changing the profile into the plane shape, it is expected that the laser-excitation processes are sufficiently saturated, so that the density ratio of Ti^+ to Ti is evaluated from the LIF intensity ratio, the ratio of the transition probabilities for the fluorescence transitions, the statistical weights of the relevant energy levels, and the sensitivity ratio of the observation system at the fluorescence wavelengths. The sensitivity ratio at the fluorescence wavelengths was evaluated experimentally using a tungsten standard lamp.

III. RESULTS

A. Density distributions of Ti^+ and Ti in vacuum

Figures 2 and 3 show the distributions of Ti^+ and Ti densities, respectively, observed in vacuum. The YAG laser pulse irradiated the target at the point of $(r,z)=(0,0)$ in the figure. The measurement delay times t_D were 0.8 and 2 μs. The absolute densities of Ti^+ and Ti were on the order of

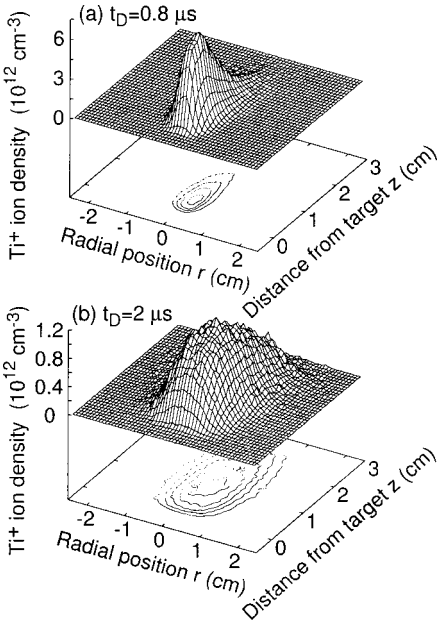

FIG. 2. Temporal variation of the density distribution of Ti^+ observed in vacuum.

10^{12} cm^{-3}. It is noted that the peak Ti^+ density was higher than the peak Ti density. On the first inspection, the density distribution shown in Fig. 2(a) suggests directional ejection of Ti^+. However, as described in the appendix, the slim distribution of the Ti^+ density at $t_D=0.8$ μs is attributed mainly to the less efficient excitation of Ti^+ in the region of $|r| \geqslant 0.5$ cm due to the Doppler effect. The ejection speed of Ti was slower than that of Ti^+ as shown in Fig. 3(a). The peak of the Ti density was adjacent to the target surface. The expansions of the density distributions were fast in vacuum. A part of the density distribution of Ti^+ was outside of the observation area at $t_D=2$ μs.

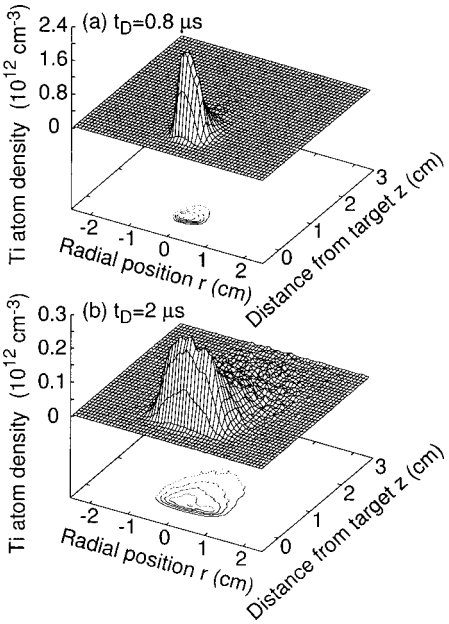

FIG. 3. Temporal variation of the density distribution of Ti observed in vacuum.

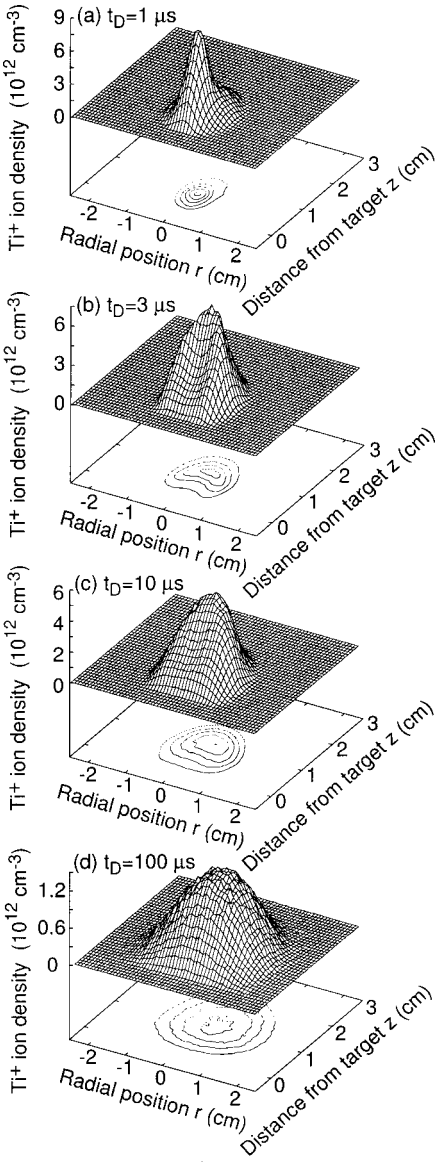

FIG. 4. Temporal variation of the density distribution of Ti^+ observed in ambient He gas at 1 Torr.

B. Density distributions of Ti^+ and Ti in ambient He gas at 1 Torr

Figures 4 and 5 show the distributions of Ti^+ and Ti densities, respectively, observed in ambient He gas at 1 Torr. In comparison with Figs. 2 and 3, the expansion speeds of Ti^+ and Ti were decelerated by collision with ambient He gas. The deceleration of the expansion speed suppressed the reduction in the excitation efficiency in the wing part of the density distributions. The less directional distribution of the Ti^+ density shown in Fig. 4(a) indicates less significant influence of the Doppler effect in the measurement. The peak of the Ti^+ density was near the leading edge of the plume at $3 \leqslant t_D \leqslant 10$ μs, which may be related to the excitation of a shock wave due to the fast expansion of the plume in ambient He gas.[5,14] At $t_D=100$ μs, the Ti^+ density had an isotropic distribution as shown in Fig. 4(d). The transport of Ti^+ at $t_D \geqslant 100$ μs was governed by diffusion.

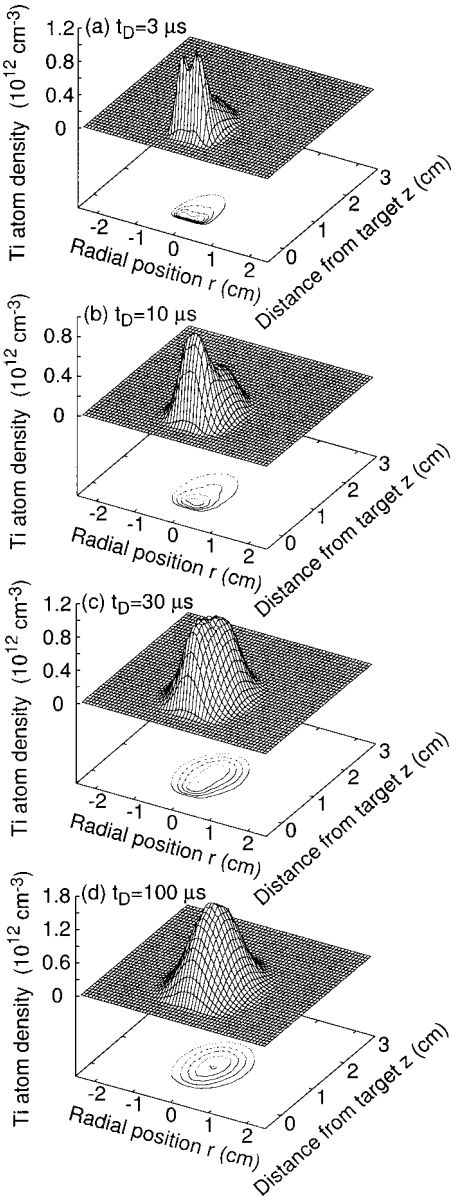

FIG. 5. Temporal variation of the density distribution of Ti observed in ambient He gas at 1 Torr.

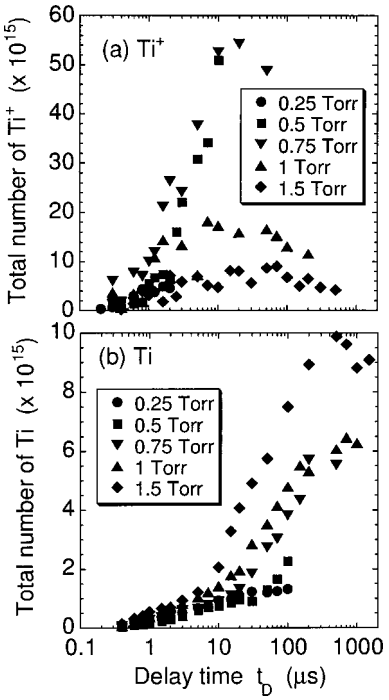

FIG. 6. Temporal variations of the total numbers of (a) Ti^+ and (b) Ti.

The Ti density in ambient He gas had twin peaks transiently as shown in Fig. 5(a). The appearance time of the twin peaks was earlier at a higher-He pressure. The distribution with the twin peaks may be owing to hydrodynamic interactions between ambient gas and particles ejected from the target. The twin peaks of the Ti density were located in the region neighboring the target surface at $t_D=3$ μs, which was in contrast to the peak position of the Ti^+ density at the same time. As seen from the magnitudes of the vertical axes of Fig. 5, the peak Ti density increased with time at $10 \leqslant t_D \leqslant 100$ μs. In addition, Figs. 5(b) and 5(c) clearly illustrate the appearance of a peak in the density distribution of Ti around $z \simeq 1$ cm from the target surface. The new peak grew with time, and became dominant at $t_D \geqslant 30$ μs. It is noted that the shift of the peak position from $z \simeq 0$ cm to $z \simeq 1$ cm is not due to the transport of Ti ejected from the target but due to the appearance of the peak. Hence, the origin of the double-peak structure shown in Fig. 5(b) is different from that observed by Wood *et al.*[15] The appearance of the peak means significant production of Ti in the gas phase around $z \simeq 1$ cm. In addition, it is emphasized that the appearance position of the peak coincides with the location of the peak Ti^+ density. Therefore, it is suggested that the gas-phase production of Ti around $z \simeq 1$ cm is attributed to neutralization of Ti^+. The Ti^+ density that is higher than the Ti density is consistent with the explanation that neutralization of Ti^+ is the source of Ti.

IV. DISCUSSION

The two-dimensional distributions of the Ti^+ and Ti densities are helpful to imagine intuitive pictures of laser-ablation plasmas. However, since the density distributions are determined by both transport and reactions, it is difficult to understand the chemical kinetics from the density distributions. To discuss the effect of reactions separately, we integrated the distributions of the Ti^+ and Ti densities spatially under the assumption of the cylindrical symmetry, so that we evaluated the temporal evolutions of the total numbers of Ti^+ and Ti included in plasmas. In the evaluation, the data were omitted when a part of the density distribution protruded from the observation area ($0 \leqslant z \leqslant 27$ mm and $-34 \leqslant r \leqslant 34$ mm).

The temporal changes in the total numbers of Ti^+ and Ti are shown in Fig. 6. The total number of Ti increased at $t_D \leqslant 500$ μs. The increase was more significant at a higher He gas pressure. In ambient He gas at 1 Torr, the total number of Ti at the maximum was observed at $t_D \simeq 500$ μs, and was approximately 100 times higher than the total number of Ti at $t_D=0.4$ μs. Although the small total number in the initial plasma is partly attributed to the low-excitation efficiency

due to the Doppler effect and quenching of the laser-excited state due to collision with ejected particles, the increase is beyond the measurement ambiguity. Since all Ti atoms in the plume are counted in this evaluation, the increase in the total number of Ti obviously means the production of Ti in the gas phase. There are no input power in laser-ablation plasmas except for the impulsive irradiation of the YAG laser beam at $t_D \leqslant 10$ ns. Considering the spatial correspondence between the location of the peak Ti^+ density and the growth region of the Ti density, neutralization of Ti^+,

$$Ti^+ + e + M \rightarrow Ti + M, \tag{1}$$

is the promising explanation for the gas-phase production of Ti. As shown in Fig. 6, the total number of Ti^+ was higher than that of Ti. Hence, from the viewpoint of the absolute numbers, neutralization of Ti^+ can be a source of Ti. Since a higher-He gas pressure (a higher density of the third body M) enhances the reaction (1), the increase in the total number of Ti is more significant at a higher pressure. The decrease in the total number of Ti at $t_D \geqslant 500$ μs may be due to the condensation of Ti to form clusters.

As shown in Fig. 6(a), we observed the temporal increase in the total number of Ti^+. The increase in the total number of Ti^+ was most significant at He gas pressures of 0.5 and 0.75 Torr. The peak time of the total number of Ti^+ appeared earlier than that of Ti. The increase in the total number of Ti^+ means the gas-phase production of Ti^+. A reasonable explanation for the gas-phase production of Ti^+ is neutralization of Ti^{2+}

$$Ti^{2+} + e + M \rightarrow Ti^+ + M. \tag{2}$$

This reaction is more efficient in a higher-He gas pressure. The lower numbers of Ti^+ observed at 1 and 1.5 Torr are attributed to the significant production of Ti from Ti^+. Since the total number of Ti^+ is determined by the balance between the production from Ti^{2+} and the loss due to neutralization (the production of Ti), the highest total number of Ti^+ is observed at pressures of 0.5 and 0.75 Torr. The experimental result showing the gas-phase production of Ti^+ suggests that multiple-charged ions are major species ejected from the target.

The present experimental results clearly indicate that ionized species are dominant in Ti plasmas produced by laser ablation of a metal Ti target at a wavelength of 1.06 μm. This is in contrast to the data obtained by Thum-Jäger and Rohr.[16] However, in laser ablation of metal targets at ultraviolet wavelengths, Hansen *et al*. and Fähler *et al*. have observed high-ionic fractions in plasmas.[17,18] The results by Hansen *et al*. and Fähler *et al*. are consistent with the present experimental results.

V. CONCLUSIONS

In the present work, we measured the distributions of the absolute Ti^+ and Ti densities in Ti plasmas produced by laser ablation of a metal Ti target. The Ti^+ and Ti densities had different distributions. Ti^+ had a faster movement speed from the target, and the peak position of the Ti^+ density was separated from the target surface. On the other hand, the peak position of the Ti density was adjacent to the target surface at the initial stage. The shift of the peak position of the Ti density was observed at $t_D \simeq 30$ μs, which was not due to the transport of Ti but due to the appearance of a peak from the gas phase. We evaluated the temporal evolutions of the total numbers of Ti^+ and Ti by integrating the density distributions spatially. As a result, it was found that the total number of Ti increased significantly after ablating the target. The increase in the total number means the gas-phase production of Ti. Considering the spatial correspondence between the peak position of the Ti^+ density and the growth

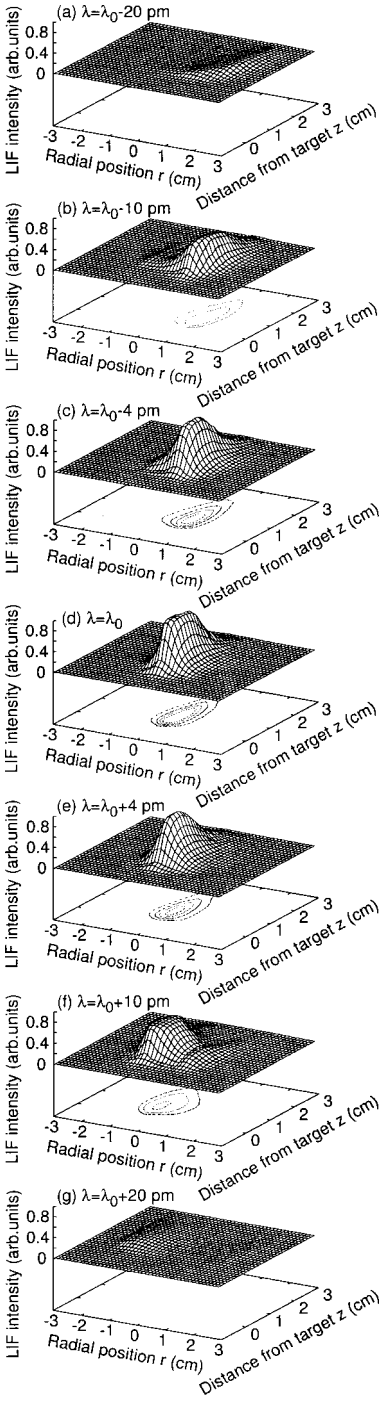

FIG. 7. Distributions of LIF intensities from Ti^+ obtained at various excitation wavelengths. This experiment was carried out in vacuum, and the measurement delay time was $t_D = 1$ μs.

region of the Ti density, neutralization of Ti^+ is the promising mechanism for the gas-phase production of Ti. The total number of Ti^+ was higher than Ti, which is consistent with the explanation that Ti^+ is the source of Ti. The total number of Ti^+ also increased at He gas pressures of 0.5 and 0.75 Torr, which may be due to neutralization of Ti^{2+}. Considering these experimental results, it is concluded that Ti^+ and Ti^{2+} are major species ejected from the metal Ti target.

ACKNOWLEDGMENT

The authors would like to thank T. Wakasaki for the assistance in the experiment.

APPENDIX

When Ti^+ and Ti have fast speed parallel to the target surface, uniform excitation in both the $r \geqslant 0$ and $r \leqslant 0$ regions is impossible. This is because the linewidth of the OPO laser ($0.25\ cm^{-1}$) was narrower than the Doppler shift. This appendix shows an example of the influence of the Doppler shift on the measurement. Figure 7 shows the LIF intensities from Ti^+ observed in vacuum at $t_D = 1\ \mu s$. This experiment was carried out using the fourth harmonics (266 nm) of a YAG laser. The experimental conditions other than the ablation wavelength were the same as those in the experiments at 1.06 μm. The center wavelength for the excitation of Ti^+ at rest is $\lambda_0 = 324.198$ nm. The various LIF intensities shown in Fig. 7 were obtained at various excitation wavelengths around λ_0. As shown in Fig. 7(d), a symmetric distribution with respect to the z axis was observed. When we shifted the excitation wavelength, LIF intensities were observed in the region where no LIF intensities were observed at the excitation wavelength of λ_0. The shift in the resonance wavelength due to the Doppler effect is given by

$$\Delta\lambda = |\lambda - \lambda_0| = \lambda_0 \left| \frac{v_r/c}{1 \pm (v_r/c)} \right| \simeq \lambda_0 (v_r/c), \tag{A1}$$

where c is the speed of light and v_r is the velocity of Ti^+ parallel to the target surface. Since Fig. 7 is obtained at $t_D = 1\ \mu s$, Ti^+ at $r = x$ cm have a parallel speed of $x \times 10^6$ cm/s, which corresponds to the Doppler shift of approximately $x \times 11$ pm. The distributions of the LIF intensities shown in Fig. 7 are consistent with the above numerical evaluation.

The speed of particles ejected from the target is decelerated in ambient gas due to collision. According to the present experimental results, the Doppler effect was negligible at $t_D \geqslant 3\ \mu s$ in ambient He gas at 0.1 Torr. In higher-He gas pressures, the Doppler effect can be ignored earlier. Hence, the temporal changes in the total numbers of Ti^+ and Ti shown in Fig. 6 are valid even if the low-excitation efficiency at the initial stage is taken into account.

[1] S. Yamamoto, T. Sumita, Sugiharuto, A. Miyashita, and H. Naramoto, Thin Solid Films **401**, 88 (2001).
[2] J.-H. Kim, S. Lee, and H.-S. Im, Appl. Phys. A: Mater. Sci. Process. **69**, S629 (1999).
[3] R. Castell, A. Ruiz, C. Casrell, and C. Suarez, Appl. Phys. A: Mater. Sci. Process. **69**, S521 (1999).
[4] I. N. Mihailescu, E. Gyorgy, N. Chitica, V. S. Teodororescu, G. Mavin, A. Luches, A. Perrone, and M. Martino, J. Mater. Sci. **31**, 2909 (1996).
[5] K. Sasaki, T. Wakasaki, S. Matsui, and K. Kadota, J. Appl. Phys. **91**, 4033 (2002).
[6] T. Okada, Mater. Sci. Forum **301**, 95 (1999).
[7] A. A. Puretzki, D. B. Geohegan, X. Fan, and S. J. Pennycook, Appl. Phys. Lett. **76**, 182 (2000).
[8] T. Ikegami, S. Ishibashi, Y. Yamagata, K. Ebihara, R. K. Thareja, and J. Narayan, J. Vac. Sci. Technol. A **19**, 1304 (2001).
[9] A. R. Striganov and N. S. Sventitskii, *Tables of Spectral Lines of Neutral and Ionized Atoms* (Plenum, New York, 1968).
[10] NIST Atomic Spectra Database, http://physics.nist.gov/cgi-bin/AtData/main_asd.
[11] T. Wakasaki, K. Sasaki, and K. Kadota, Jpn. J. Appl. Phys., Part 1 **41**, 5792 (2002).
[12] A. G. Mitchell and M. W. Zemansky, *Resonance Radiation and Excited Atoms* (Cambridge University, Cambridge, England, 1961) p. 92.
[13] S. Matsui, T. Wakasaki, K. Sasaki, and K. Kadota, J. Plasma Fusion Res. **76**, 1165 (2000) [in Japanese].
[14] Ya. B. Zel'dovich and Yu. P. Raizer, "*Physics of Shock Waves and High Temperature Hydrodynamic Phenomena* (Academic Press, New York, 1966).
[15] R. F. Wood, K. R. Chen, J. N. Leboeuf, A. A. Puretzky, and D. B. Geohegan, Phys. Rev. Lett. **79**, 1571 (1997).
[16] A. Thum-Jäger and K. Rohr, J. Phys. D **32**, 2827 (1999).
[17] T. N. Hansen, J. Schou, and L. G. Lunney, Europhys. Lett. **40**, 441 (1997).
[18] S. Fähler, K. Sturm, and H.-U. Krebs, Appl. Phys. Lett. **75**, 3766 (1999).